Axisymmetric Stagnation Flow and Heat Transfer of a Compressible Fluid Impinging on a Cylinder Moving Axially

Asghar B. Rahimi[1]
Professor
Faculty of Engineering,
Ferdowsi University of Mashhad,
P. O. Box No. 91775-1111,
Mashhad 1111, Iran
e-mail: rahimiab@yahoo.com

Hamid Mohammadiun
Assistant Professor
Department of Mechanical Engineering,
Shahrood Branch,
Islamic Azad University,
Shahrood 3619633619, Iran.

Mohammad Mohammadiun
Assistant Professor
Department of Mechanical Engineering,
Shahrood Branch,
Islamic Azad University,
Shahrood 3619633619, Iran

The steady-state viscous flow and also heat transfer in the vicinity of an axisymmetric stagnation point on a cylinder moving axially with a constant velocity are investigated. Here, fluid with temperature-dependent density is considered. The impinging freestream is steady and with a constant strain rate (strength) $\bar{k}$. An exact solution of the Navier–Stokes equations and energy equation is derived in this problem. A reduction of these equations is obtained by use of appropriate transformations. The general self-similar solution is obtained when the wall temperature of the cylinder or its wall heat flux is constant. All the solutions above are presented for Reynolds numbers, $Re = \bar{k}a^2/2\upsilon$, ranging from 0.1 to 1000, low Mach number, selected values of compressibility factor, and different values of Prandtl numbers where a is cylinder radius and υ is kinematic viscosity of the fluid. Shear stress is presented as well. Axial movement of the cylinder does not have any effect on heat transfer but its increase increases the axial component of fluid velocity field and the shear stress. [DOI: 10.1115/1.4031130]

Keywords: stagnation flow, viscous compressible fluid, low Mach number, heat transfer, moving cylinder, exact solution, constant wall temperature, heat flux

1 Introduction

Axial movement of a cylinder in the case of stagnation-point flow and heat transfer has many applications in manufacturing processes. For example, the cooling processes or cleaning processes of punching instruments and drilling tools are the sample of industrial applications. The following picture may best describe how a radial flow can be arranged in order to coat the surface of a cylinder with any kind of protection material. This coating can be considered as protection against erosion or for the purpose of insulation. The flow on the cylinder is coming from all directions.

Existing solutions of the problem of axisymmetric stagnation-point flow and heat transfer on either a cylinder or a flat plate are for viscous, incompressible fluid. These studies started by Hiemenz [1] who obtained an exact solution of the Navier–Stokes equations governing the two-dimensional stagnation-point flow on a flat plate and went on by Homann [2] which was an analogous axisymmetric study, and by Howarth [3] and Davey [4] where results for stagnation flow against a flat plate for axisymmetric cases were presented. Wang [5,6] was first to find an exact solution for the problem of axisymmetric stagnation flow on an infinite stationary circular cylinder and continued by Gorla [7–11] which are a series of steady and unsteady flows and heat transfer over a circular cylinder in the vicinity of the stagnation point for the cases of constant axial movement and the special case of axial harmonic motion of a nonrotating cylinder. Cunning et al. [12] have considered the stagnation flow problem on a rotating circular cylinder with constant angular velocity, and Grosch et al. [13] and Takhar et al. [14] who studied special cases of unsteady viscous flow on an infinite circular cylinder. The more recent works of the same types are the ones by Saleh and Rahimi [15] and Rahimi and Saleh [16,17] which are exact solution studies of a stagnation-point flow and heat transfer on a circular cylinder with time-dependent axial and rotational movements, and studies by Shokrgozar and Rahimi [18–22] are exact solutions of stagnation-point flow and heat transfer but on a flat plate. Fluid flow and Miaxed convection transport from a Plate in a rolling and extrusion process have been studied by Karwe and Jaluria [23]; in this research, the heat transfer arising due to the movement of a continuous heated plate in processes such as hot rolling and hot extrusion has been studied. Kang et al. [24] have experimentally investigated the convective cooling of a heated continuously moving material. They considered the effects of thermal buoyancy, material speed, and properties of the material and the fluid on the thermal field. Forced convection heat transfer from a continuously moving heated cylindrical rod in materials processing has been considered by Choudhury and Jaluria [25]. They presented numerical solutions to the vorticity, temperature, and stream function equations in cylindrical coordinate system and another numerical simulation of continuously moving flat sheet has been presented by Karwe and Jaluria [26]. Recently, the results of axisymmetric stagnation flow of incompressible fluid on a heated vertical plate with surface slip and annular axisymmetric stagnation flow on a moving cylinder have been reported by Hong and Wang [27,28]. Useful information in the area of stagnation point flow in the CVD reactor has been experimentally extracted by Memon and Jaluria [29]. This experimental research will be used to understand the buoyancy induced and momentum driven flow structure encountered in an impinging jet CVD reactor.

Magnetohydrodynamic stagnation point flow of second grade fluid over a permeable stretching cylinder has been studied by Hayat et al. [30]. They used suitable transformations to convert nonlinear partial differential equations into the nonlinear ordinary differential equations. In this research, variation of different parameters on the velocity, temperature, and concentration profiles have been shown graphically. They also computed numerical values of skin friction coefficient, Nusselt number and Sherwood number. An adaptive mesh strategy for high compressible flows based on nodal re-allocation has been presented by Bono and Awruch [31]. The development of a simple and computationally effective methodology to adapt finite-element meshes to simulate compressible flows with strong shock waves was the main objective of their work. The nodal re-allocation adaptivity, used in this

[1]Corresponding author.

Contributed by the Heat Transfer Division of ASME for publication in the Journal of Heat Transfer. Manuscript received March 2, 2014; final manuscript received July 15, 2015; published online October 6, 2015. Assoc. Editor: William P. Klinzing.

research, starts from an initial mesh and the grids are concentrated in the desired region without any grid tangling.

Some existing compressible flow studies but in the stagnation region of bodies and by using boundary layer equations include the study by Subhashini and Nath [32] as well as Kumari and Nath [33,34], which are in the stagnation region of a body, and work of Katz [35] as well as Afzal and Ahmad [36], Libby [37], and Gersten et al. [38], which are all general studies in the stagnation region of a body. Existing compressible flow studies are all general studies in the stagnation region of a body and by using boundary layer equations. Stagnation point flow and heat transfer of a viscous, compressible fluid on a flat plate have been investigated by Mozayyeni and Rahimi [39,40].

The only study that deals with stagnation-point flow and heat transfer of a viscous fluid, with temperature-dependent density on a cylinder is by Mohammadiun and Rahimi [41]. They obtained an exact solution of the Navier–Stokes equations for the case of a stationary cylinder.

The problem of stagnation-point flow and heat transfer for the case of temperature-dependent density when the cylinder is moving axially has not been considered so far. In this research work, solution of the problem of axisymmetric stagnation-point flow and heat transfer is presented for the case of compressible, viscous fluid on a cylinder when it is moving axially with a constant velocity. An exact solution of the Navier–Stokes equations and the energy equation is obtained. The self-similar solution is reached by introducing the appropriate similarity variables. Sample distributions of shear stress and temperature fields at Reynolds numbers ranging from 0.1 to 1000 are presented for different values of Prandtl numbers and fluid compressibility factor. The compressibility factor and Mach number have been considered in the ranges of 0–0.09 and 0.01–0.1, respectively, and Prandtl number from 0.1 to 1. Because of these restrictions, the radial velocities approaching the cylinder should be assumed in the range of 3.4 m/s to 34 m/s.

2 Problem Formulation

Flow and its schematic mechanism is considered in cylindrical coordinates (r, φ, z) with corresponding velocity components (u, v, w); see Figs. 1 and 2. We consider the steady-state laminar flow of a viscous, compressible fluid along with heat transfer in the neighborhood of an axisymmetric stagnation point of an infinite circular cylinder moving with a constant axial velocity. An external axisymmetric radial stagnation flow of strain rate $\bar{k}$ impinges on the cylinder of radius a, centered at $r = 0$. To introduce the strain rate $\bar{k}$, it must be referred to solution of the inviscid flow at the so far distance from the cylinder that it is obtained by using the continuity equation as follows. Considering Fig. 3:

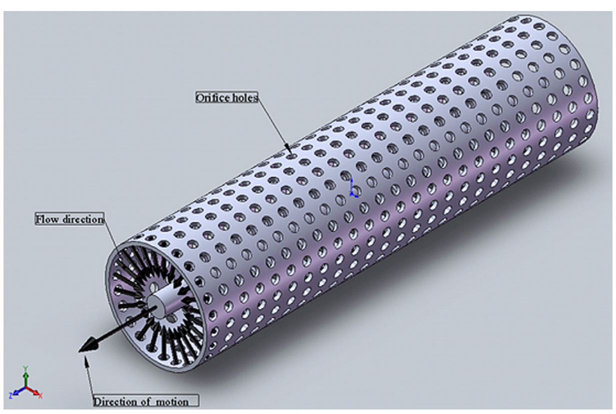

Fig. 1 A schematic mechanism of the radially impinging flow production

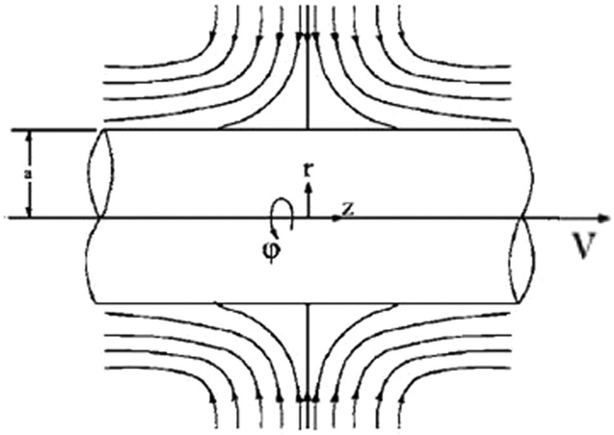

Fig. 2 Schematic diagram of an axially moving cylinder

Start from continuity equation

$$r \to \infty: \frac{\partial(\rho U)}{\partial r} + \frac{\rho U}{r} + \frac{\partial(\rho w)}{\partial z} = 0\,,$$
$$(\rho = \rho_\infty) \Rightarrow \frac{\partial U}{\partial r} + \frac{U}{r} + \frac{\partial w}{\partial z} = 0 \Rightarrow \frac{1}{r}\frac{\partial}{\partial r}(rU) + \frac{\partial w}{\partial z} = 0 \tag{1}$$

Transferring the term $(\partial w/\partial z)$ to the other side of the equation and considering $(1/r)(\partial/\partial r)(rU)$ is the only function of r and $(\partial w/\partial z)$ is the only function of z, this equality will be achieved if it equals the constant value. According to the above explanations, the following results are obtained:

$$-\frac{1}{r}\frac{\partial}{\partial r}(rU) = \frac{\partial w}{\partial z} = C_1 = 2\bar{k} \tag{2}$$

In the above equation, $\bar{k}$ is a constant value that is called strain rate of the stagnation point flow.

Also, Reynolds number is obtained after changing the momentum equations in the dimensionless form. For example, referring the dimensionless equations of radial and axial momenta, it is observed that the term of $(ka^2/2\upsilon)$ is appeared in both equations.

The steady Navier–Stokes and energy equations in cylindrical polar coordinates governing the axisymmetric compressible flow and heat transfer, neglecting the body force and also neglecting the variation of viscosity, conductivity, and specific heat with temperature are as follows:

Mass

$$\frac{\partial(\rho u)}{\partial r} + \frac{\rho u}{r} + \frac{\partial(\rho w)}{\partial z} = 0 \tag{3}$$

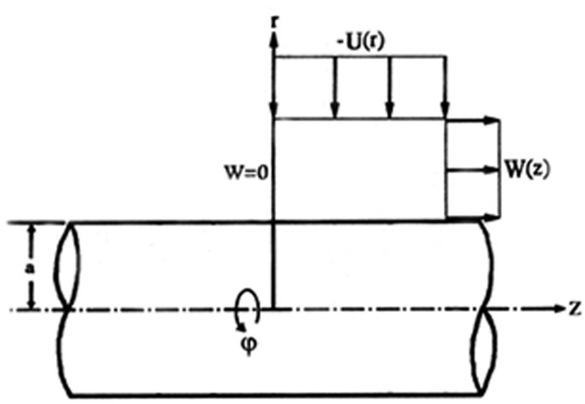

Fig. 3 Schematic diagram of inviscid flow on cylinder

r-momentum

$$u\frac{\partial(\rho u)}{\partial r}+w\frac{\partial(\rho u)}{\partial z}=-\frac{\partial P}{\partial r}+\upsilon\left\{\frac{1}{r}\frac{\partial}{\partial r}\left[r\frac{\partial(\rho u)}{\partial r}\right]-\frac{(\rho u)}{r^2}+\frac{\partial^2(\rho u)}{\partial z^2}\right\} \tag{4}$$

z-momentum

$$u\frac{\partial(\rho w)}{\partial r}+w\frac{\partial(\rho w)}{\partial z}=-\frac{\partial P}{\partial z}+\upsilon\left\{\frac{1}{r}\frac{\partial}{\partial r}\left[r\frac{\partial(\rho w)}{\partial r}\right]+\frac{\partial^2(\rho w)}{\partial z^2}\right\} \tag{5}$$

and energy

$$\rho u\frac{\partial T}{\partial r}+\rho w\frac{\partial T}{\partial z}=\frac{\mu}{\Pr}\frac{1}{r}\frac{\partial}{\partial r}\left(r\frac{\partial T}{\partial r}\right) \tag{6}$$

In these equations P, ρ, υ, and T are the fluid pressure, density, kinematic viscosity, and temperature. The boundary conditions for velocity field are

$$r=a: \quad u=0,\ w=V \tag{7}$$

$$r\to\infty:\ u=-\bar{k}(r-a^2/r), \quad w=2\bar{k}z \tag{8}$$

In which, Eq. (7) is the no-slip condition on the cylinder wall and V is the axial velocity of the cylinder. Relations (8) show that the viscous flow solution approaches, in a manner analogous to the Hiemenz flow, the potential flow solution as $r\to\infty$, Ref. [12].

For the temperature field we have

$$r=a:\begin{cases} T=T_w=\text{cons}\tan\text{t}, & \text{for defined wall temperature (Dirichlet b.c)}\\ \dfrac{\partial T}{\partial r}=-\dfrac{q_w}{k}, & \text{for defined wall heat flux (Neu mann b.c)}\end{cases}$$
$$r\to\infty: \quad T\to T_\infty \tag{9}$$

In the above relations, k is the thermal conductivity of the fluid and T_w and q_w are temperature and heat flux at the cylinder wall, respectively, and T_∞ is the freestream temperature.

A reduction of the Navier–Stokes equations is obtained by the following coordinate separation of the velocity field

$$u=-\frac{\bar{k}a^2}{r}\frac{\rho_\infty}{\rho(\eta)}f(\eta),\ w=\frac{\rho_\infty}{\rho(\eta)}\left[2\bar{k}cf'(\eta)z+H(\eta)\right],\ p=\rho_\infty\bar{k}^2a^2P \tag{10}$$

where

$$\eta=\frac{2}{a^2}\int_a^r\frac{\rho r}{\rho_\infty}dr \quad \left(\eta=\frac{r^2-a^2}{a^2}\quad \text{for } \rho=cons\tan t\ \&\ \beta=0\right) \tag{11}$$

Here, η is dimensionless radial variable, Ref. [41], and prime denotes differentiation with respect to η, and ρ_∞ is freestream density. For the case of incompressible flow ($\rho(\eta)$ =constant), this variable is similar to the one in Wang (Ref. [5]) except that it changes from zero to infinity instead of one to infinity. This similarity variable has been extracted by refer to the dimensionless variable which is used in the vicinity of axisymmetric stagnation point of incompressible fluid. Because of the variation in fluid density and by use of similar patterns in compressible fluid, dimension less density (ρ/ρ_∞) has been used to the definition of the similarity variable. Velocity components of viscous fluid have been achieved by refer to the inviscid solution at the so far distance from cylinder and multiplying the velocity component of inviscid fluid by the functions of η. These functions have been extracted by trial and error.

Transformations (10) satisfy Eq. (3) automatically and their insertion into Eqs. (4) and (5) yields a coupled system of differential equations in terms of $f(\eta)$, $H(\eta)$, and an expression for the pressure

$$\Gamma[c^3f'''+3c^2c'f''+c^2c''f'+(c')^2cf']+c^2f''+cc'f'$$
$$+\text{Re}[1+c'ff'+cff''-c(f')^2]=0 \tag{12}$$

$$\Gamma(c^2H''+cc'H')+cH'+\text{Re}(fH'-f'H)=0 \tag{13}$$

$$p-p_0=\int_0^\eta\left[\frac{1}{2}\left(\frac{f}{\Gamma c}\right)^2-\frac{ff'}{\Gamma c^2}-\frac{1}{\text{Re}}(cf')\right]d\eta-2\left(\frac{z}{a}\right)^2 \tag{14}$$

In these equations, $c(\eta)=\rho(\eta)/\rho_\infty$, $\text{Re}=\bar{k}a^2/2\upsilon$, $\Gamma(\eta)=1+\int_0^\eta d\eta/c(\eta)$, and prime indicates differentiation with respect to η. From conditions (7) and (8), the boundary conditions for Eqs. (12) and (13) are as follows:

$$\begin{aligned}&\eta=0: \quad f=0,\quad f'=0,\quad H=Vc(0)\\ &\eta\to\infty:\ f'=1,\quad H=0\end{aligned} \tag{15}$$

To model the variation of density with respect to temperature, the following Boussinesq approximation is used assuming low Mach number flow:

$$\rho\approx\rho_\infty[1-\beta(T-T_\infty)]\Rightarrow\ \rho/\rho_\infty=c(\eta)=1-\beta(T-T_\infty) \tag{16}$$

In the above relation, ρ_∞ and β are freestream density and compressibility factor, respectively. To transform the energy equation into a nondimensional form, we introduce

$$\theta(\eta)=\begin{cases}\dfrac{T(\eta)-T_\infty}{T_w-T_\infty}, & \text{for the case of defined wall temperature}\\ \dfrac{T(\eta)-T_\infty}{\dfrac{aq_w}{2k}}=\dfrac{T(\eta)-T_\infty}{\gamma}, & \text{for the case of defined wall heat flux}\end{cases} \tag{17}$$

where $\gamma = a\,q_w/2k$ is used in figures and presented results.

Making use of Eqs. (10) and (17) the energy equation may be written as

$$\frac{1}{\mathrm{Re.Pr}}\left[\Gamma(c^2\,\theta'' + cc'\theta') + c\theta'\right] + f\theta' = 0 \tag{18}$$

With boundary conditions as

$$\begin{aligned}
&\eta = 0: \begin{cases} \theta = 1, & \text{for the case of defined wall temperature} \\ -\theta'\left[1 - \beta\left(\dfrac{a\,q_w}{2k}\right)\right] = 1, & \text{for the case of defined wall heat flux} \end{cases} \\
&\eta \to \infty:\ \ \theta = 0, \qquad \text{for both cases}
\end{aligned} \tag{19}$$

The local Nusselt number is given by

$$\mathrm{Nu} = \frac{h\,a}{2k} = \begin{cases} -\theta'(0)\,c(0), & \text{for the case of defined wall temperature} \\ \dfrac{1}{\theta(0)}, & \text{for the case of defined heat flux} \end{cases} \tag{20}$$

Because of $c(\eta)$, Eqs. (12)–(14), and (18) are dependent. Note that for the case of incompressible fluid $\rho(\eta) = \rho_\infty$ Eq. (12) is exactly reduced to the equation obtained by Wang in Ref. [5] for radial component of the velocity and also Eq. (18) reduces to the equation obtained by Gorla in Ref. [7], with consideration of starting value for the variable η.

3 Shear Stress

Assuming the cylinder is infinite and considering that any one of the boundary conditions is not the function of z-axis, so the velocity profile of u cannot be a function of z; thus, $u = u(r, \phi)$ In addition, due to an axial symmetry: $\partial u/\partial\phi = 0 \Rightarrow u(r)$ for the shear stress on the surface of the cylinder is obtained from

$$\sigma = \mu\left[\frac{\partial u}{\partial z} + \frac{\partial w}{\partial r}\right]_{r=a} \quad \text{or} \quad \sigma = \mu\left[\frac{\partial w}{\partial r}\right]_{r=a}$$

but

$$\frac{\partial w}{\partial r} = \frac{\partial w}{\partial \eta}\frac{\partial \eta}{\partial r} = \left[2\bar{k}f''\,z + \frac{H'}{c(\eta)} - \frac{Hc'}{c(\eta)^2}\right]\frac{2r}{a^2}c(\eta) \tag{21}$$

Since $\eta = 0$ at $r = a$, then we have

$$\sigma = \mu\left[2\bar{k}f''(0)\,z + \frac{H'(0)}{c(0)} - \frac{H(0)\,c'(0)}{c^2(0)}\right]\frac{2}{a}c(0) \tag{22}$$

As the governing equations show, considering compressibility effect causes the momentum equations and the energy equation to be coupled together which helps the designer to control the velocity gradient on the surface by varying this compressibility factor which eventually affects the shear stress.

Results of $|\sigma\,a/2\mu|_{z=0}$ for different values of Re with Pr held constant and for different values of Pr with Re held constant are presented in Sec. 5.

4 Numerical Procedures

Equations (12)–(14), and (18) along with boundary conditions (15) and (19) are solved by using the fourth-order Runge–Kutta method along with shooting technique [42]. Using this method, the initial values are guessed and the integration is repeated until convergence is obtained. In these computations, the step size in η-direction is optimized and $\Delta\eta = 0.001$ and $\eta_{\max} = 15$ are used throughout computations. The truncation error was set at 1×10^{-9}. The obtained results (H/V and $\hat{\psi}$) are compared with reliable source [28] to examine the accuracy of numerical solution method. Comparison of dimensionless axial movement function (H/V) and the normalized stream function $\hat{\psi}$ with the results from Ref. [28] has been done. All of the results have been extracted for the case of incompressible fluid ($\beta = 0$). The results have been calculated for ($\alpha = V/\bar{k}\,a = 3$) and in the case of stationary cylinder ($\alpha = 0$). In each case there is a good conformity between the presented results and the results from Ref. [28]. As expected when the cylinder moves axially, the symmetric stream lines are converted into skewed shape and the stagnation point of the fluid is moved down to negative values of z/a.

5 Results and Discussion

In this section, the solution of the self-similar Eqs. (12), (13), and (18) along with the surface shear stresses for prescribed values of surface temperature and heat flux and at selected values of Reynolds and Prandtl numbers are presented. It should be noted the flow filed as drawn in Fig. 2 only pertains to regions beyond the boundary layer. Equations (12), (14), and (18) are the same as in Ref. [41] which is for a stationary cylinder. Meaning that the axial movement of the cylinder represented by H appears neither in the equation for the radial velocity f nor in the energy equation. Radial component of velocity will change with the modification of the radial momentum, but cylindrical axial velocity only causes the increase of the axial momentum and has no effect on the radial momentum. Therefore, cylindrical axial movement has no effect on the radial velocity component and also heat transfer.

As mentioned previously, stagnation-point flow can be used in cleaning of drills and different cutting tools, for example. In this application, the effect of surface shear stress plays a great role since removing the unwanted materials from tools surface has a direct relationship with its increase. Presented results show how the increase of compressibility of fluid produces a greater surface shear stress and also how with increase of surface temperature or heat flux the removal of the excess materials can take place easier.

5.1 Influence of Prandtl Number.

Sample profiles of variation of dimensionless axial movement function (H/V) against η for compressibility factor $\beta = 0.0033$ and for selected values of Prandtl numbers are presented in Fig. 4 as Dirichlet boundary condition and Fig. 5 as Neumann boundary condition. Constant wall temperature $T_w = 500$K, freestream temperature $T_\infty = 300$ K,

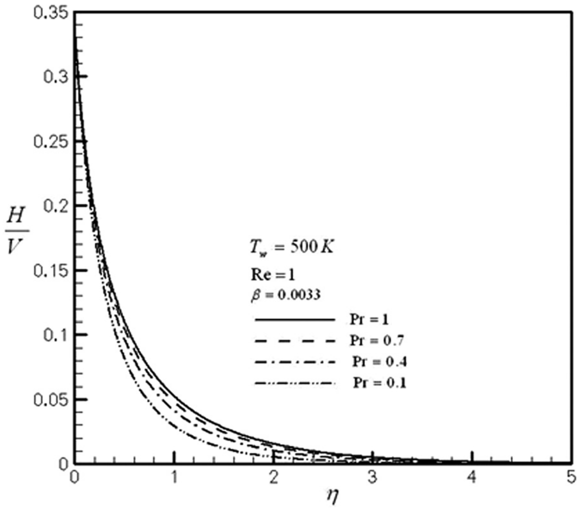

Fig. 4 Variation of dimensionless axial movement function (H/V) in terms of η for $T_w = 500\,\mathrm{K}$, $T_\infty = 300\,\mathrm{K}$, $\beta = 0.0033$, Re = 1, and selected values of Prandtl number

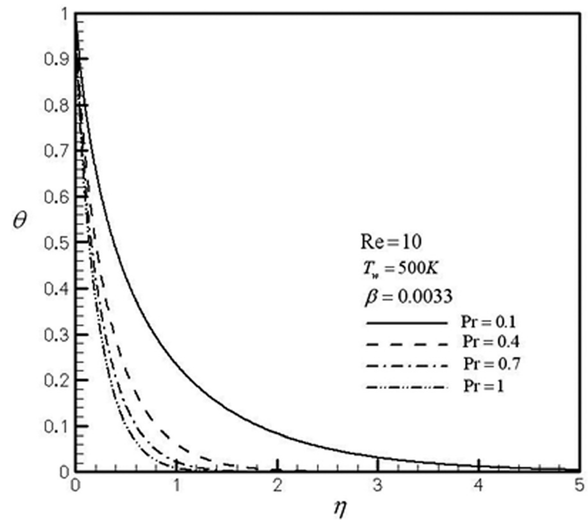

Fig. 6 Variation of θ in terms of η at, $T_w = 500\,\mathrm{K}$, $T_\infty = 300\,\mathrm{K}$, Re = 10.0, $\beta = 0.0033$, and for different values of Prandtl numbers

Reynolds number $\mathrm{Re} = 1$ and constant wall heat flux index $\gamma = 100$, Reynolds number $\mathrm{Re} = 10$ are used to extract these profiles, respectively. In each case as Prandtl number increases the depth of diffusion of defined function (H/V) increases which means that the axial component of the fluid velocity field for a specified axial velocity of the cylinder increases as Pr number increases and also this increase is larger when cylinder moves faster.

Effect of Prandtl number variation on dimensionless temperature $\theta(\eta)$ for the case of constant wall temperature for compressibility factor $\beta = 0.0033$, $\mathrm{Re} = 10$, $T_\infty = 300\,\mathrm{K}$, and $T_w = 500\,\mathrm{K}$ or $\gamma = 10$ is shown in Fig. 6. As expected by increasing the Prandtl number, the depth of energy diffusion decreases against the depth of momentum diffusion and this reduction in the depth of energy diffusion leads to reduction in the thermal boundary layer thickness and therefore the temperature gradient on the wall and local heat transfer coefficient increase. Same type of information can be extracted for the case of constant wall heat flux.

5.2 Influence of Compressibility Factor. The effects of changing compressibility factor on dimensionless axial movement function (H/V) against η for $T_w = 500\,\mathrm{K}$, $\mathrm{Pr} = 1$ and Reynolds number $\mathrm{Re} = 100$ are depicted in Fig. 7. For each value of Reynolds number as the compressibility factor increases the fluid density decreases and this reduction in fluid density leads to reduction in the axial momentum which means that the axial component of the fluid velocity field for a specified axial velocity of the cylinder decreases as the compressibility factor increases and also this decrease is larger when the cylinder moves faster.

According to the relations $H(0) = V\,c(0)$ & $c(0) = 1 - \beta(T_w - T_\infty)$, it is determined that by increasing the compressibility factor β, $c(0)$ decreases, and since V is fixed, $H(0)$, and consequently $H(0)/V$ decrease too. This can be physically justified: by changing the compressibility factor, fluid density changes that it causes the modification of the dynamic viscosity of the fluid, and this variation in the dynamic viscosity leads to variation in the axial momentum diffusion.

It is worth mentioning that in each case the incompressible fluid produces the largest amount of change in axial component of the fluid velocity field. In each case the incompressible fluid ($\beta = 0$) has been compared with the results of Gorla [9], which shows suitable match. It is also noted that as Reynolds number increases, because of increasing the radial momentum of the fluid, the effect of cylinder movement on axial velocity component of the fluid decreases. Same type of information can be gathered for a specified cylinder surface heat flux.

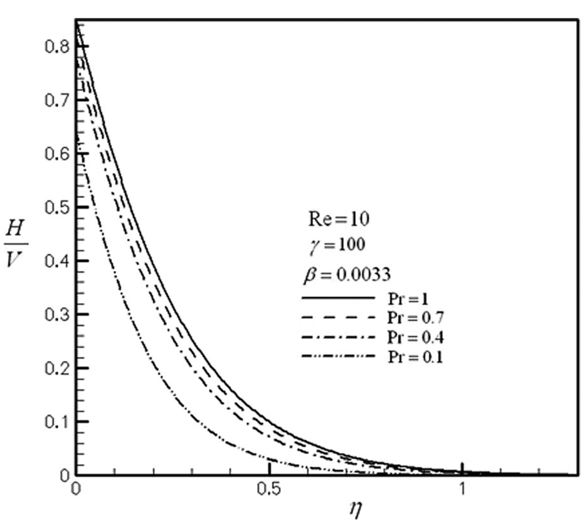

Fig. 5 Variations of dimensionless axial movement function (H/V) in terms of η for selected values of Pr for Re = 10, $\beta = 0.0033$, and $\gamma = 100$

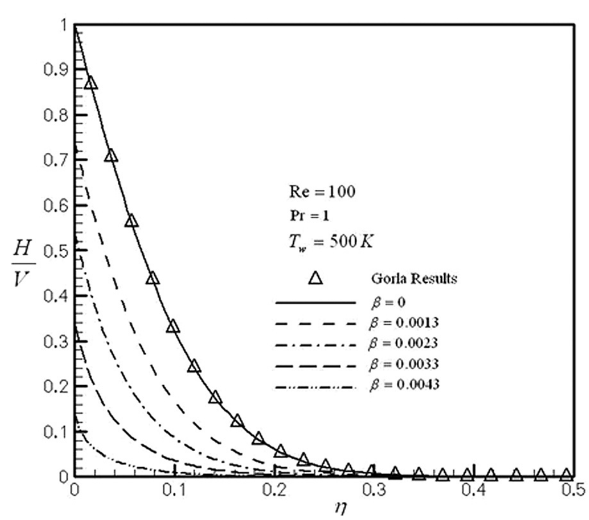

Fig. 7 Variations of dimensionless axial movement function (H/V) in terms of η for selected values of β for Re = 100, Pr = 1, and $T_w = 500\,\mathrm{K}$

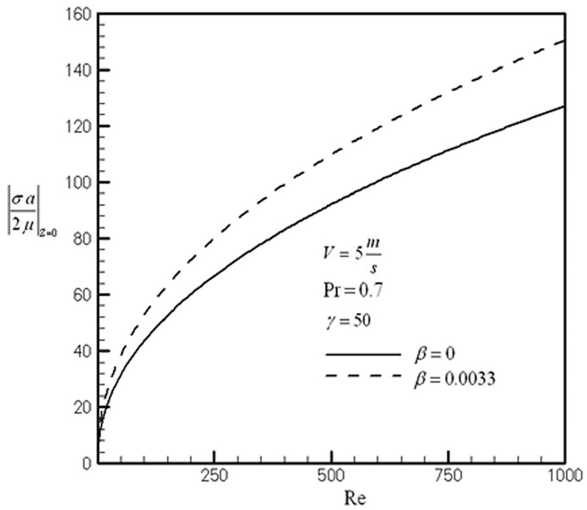

Fig. 8 Variation of shear stress versus Reynolds number at Pr = 0.7, γ = 50, V = 5 m/s for selected values of compressibility factor

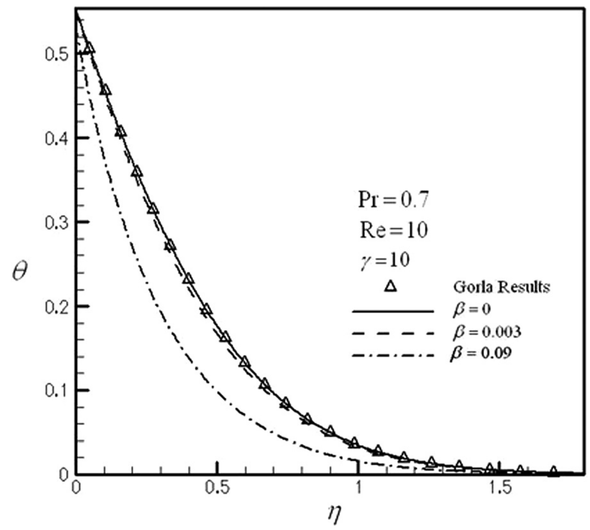

Fig. 10 Variations of θ in terms of η at γ = 10.0 and Pr = 0.7, Re = 10 for different values of compressibility factor

Influence of compressibility factor on wall shear stress has been shown in Fig. 8. By comparing these profiles, it can be found that, because of increasing in the velocity boundary layer thickness and reduction in the velocity gradient on the surface, the incompressible fluid case produces the least amount of wall shear stress.

Effect of variations of compressibility factor on dimensionless temperature $\theta(\eta)$ against η for $T_w = 500\,\mathrm{K}$, $\mathrm{Pr} = 1.0$, and selected value of Reynolds numbers are presented in Fig. 9. For $\beta = 0$, incompressible fluid, the result of Gorla [7] is extracted and it is interesting to note that as β increases the depth of the diffusion of the thermal boundary layer decreases. Same type of information can be gathered from Fig. 10 but for a specified cylinder surface heat flux.

5.3 Influence of Reynolds Number. Changes of wall shear-stress versus wall temperature or wall heat flux are shown in Figs. 11 and 12 for different axial cylinder speed and selected values of Reynolds numbers. As can be seen from these figures, the absolute value of shear stress increases with Reynolds number, wall temperature, and wall heat flux or cylinder axial speed. In each case because of increasing the velocity gradient on the cylinder wall the shear stress increases.

Sample profiles of pressure function against η for the case of $\mathrm{Pr} = 0.7$, $T_w = 500\,\mathrm{K}$, $\beta = 0.0033$, and for selected values of Reynolds numbers are shown in Fig. 13. As expected, by increase of Reynolds number the depth of diffusion of fluid pressure increases.

Sample profiles of the $f(\eta)$ function against η for compressibility factor, $\beta = 0.0033$, $\mathrm{Pr} = 0.7$, constant wall temperature $T_w = 300\,\mathrm{K}$ and for selected values of Reynolds numbers are presented in Fig. 14 (same type of graph can be produced for the case of constant wall heat flux). Since the increase of Reynolds number causes the dynamic inertia forces to overcome the viscous forces, as expected like the behavior of the incompressible fluid, the depth of diffusion of the momentum increases. So as the Reynolds number increases, the radial velocity field increases, too.

5.4 Influence of Wall Temperature or Wall Heat Flux. Changes of wall shear stress versus Reynolds number for selected values of wall temperature are shown in Fig. 15 (same type graph can be presented for the case of wall heat flux) for defined axial cylinder speed. As it can be seen from this figure the absolute value of wall shear stress increases with the Reynolds number, wall temperature, or wall heat flux, because of increasing in the velocity gradient on the cylinder surface.

Finally, the variations of dimensionless axial movement function and its comparison with Wang's results and the normalized stream functions have been represented in Figs. 16–18, respectively.

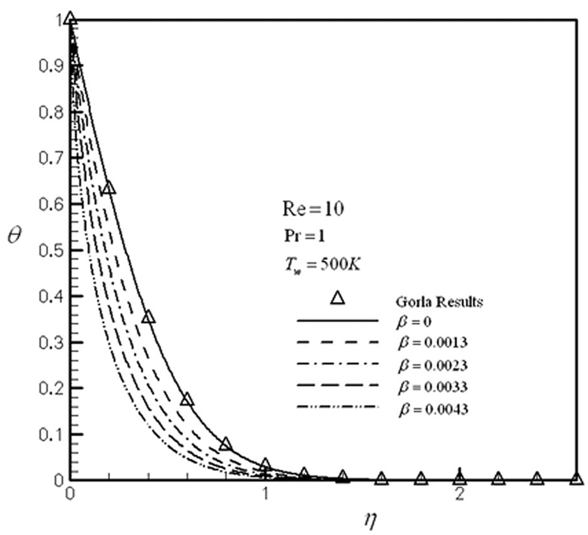

Fig. 9 Variations of θ in terms of η at Pr = 1.0, T_w = 500 K, T_∞ = 500 K, Re = 1.0, and for different values of compressibility factor

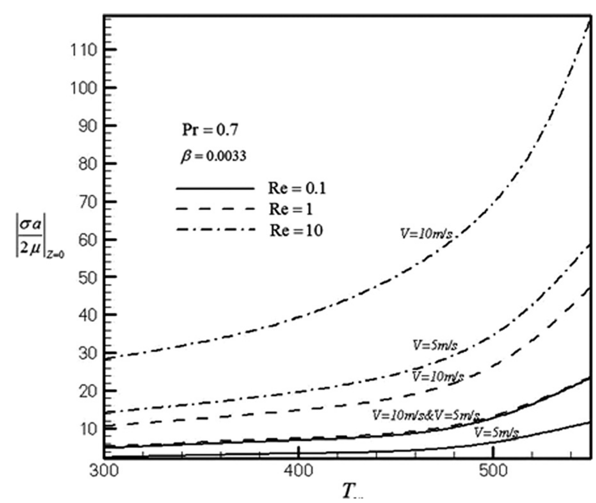

Fig. 11 Variation of shear stress against wall temperature at V = 5 m/s and V = 10 m/s, Pr = 0.7, β = 0.0033, and for selected values of Reynolds numbers

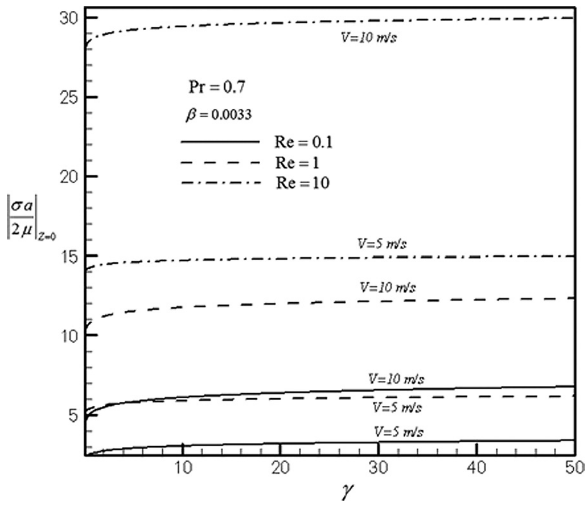

Fig. 12 Variation of shear stress against γ for selected values of Reynolds number at $V = 5\,\mathrm{m/s}$ and $V = 10\,\mathrm{m/s}$, Pr = 0.7, $\beta = 0.0033$, and for selected values of Reynolds number

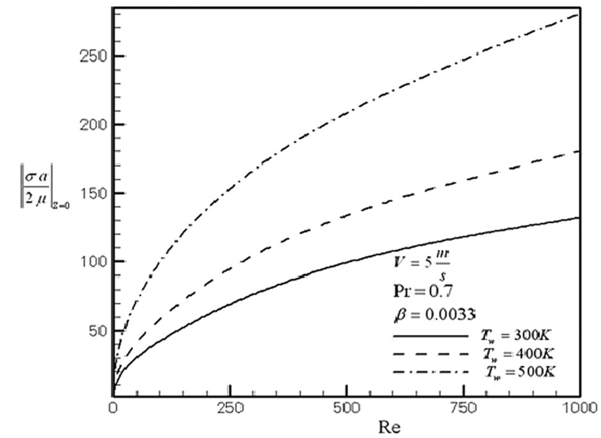

Fig. 15 Variation of shear stress against Reynolds number at $V = 5\,\mathrm{m/s}$, Pr = 0.7, $\beta = 0.0033$, and for selected values of wall temperature

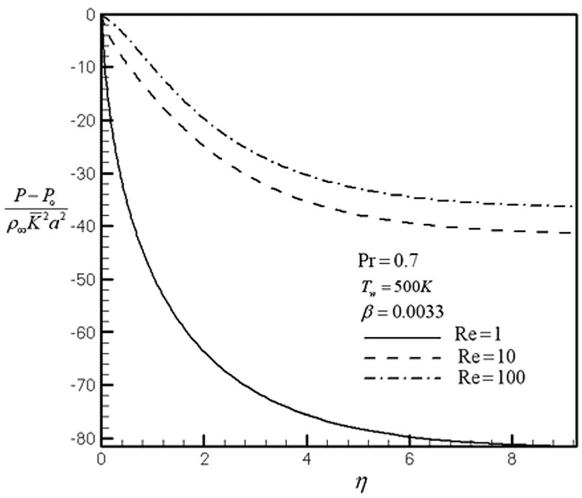

Fig. 13 Variation of pressure function in terms of η at, Pr = 0.7, $T_w = 500\,\mathrm{K}$, $T_\infty = 300\,\mathrm{K}$, $\beta = 0.0033$, and for different values of Reynolds numbers

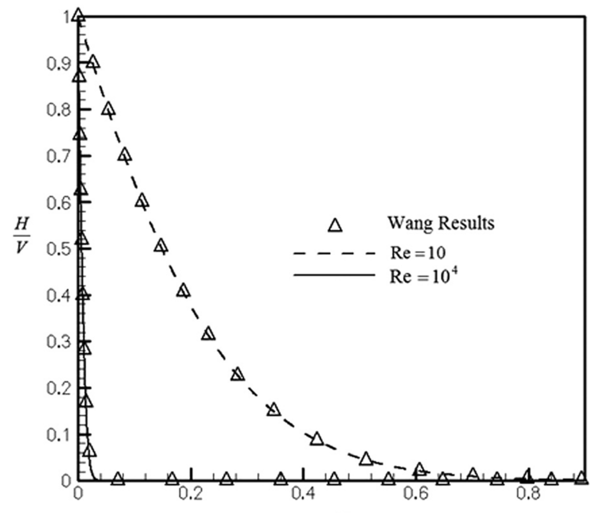

Fig. 16 Variations of dimensionless axial movement function (H/V) in terms of η for $\beta = 0$ and for selected values of Reynolds number

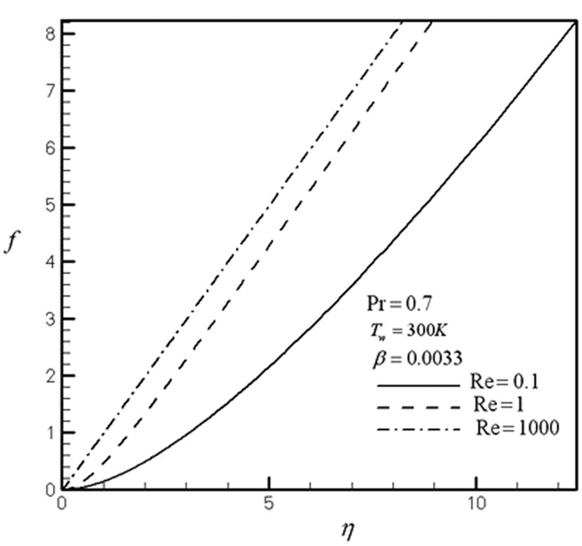

Fig. 14 Variation of f in terms of η at $T_w = 300\,\mathrm{K}$, $\beta = 0.0033$, and Pr = 0.7 for different values of Reynolds numbers

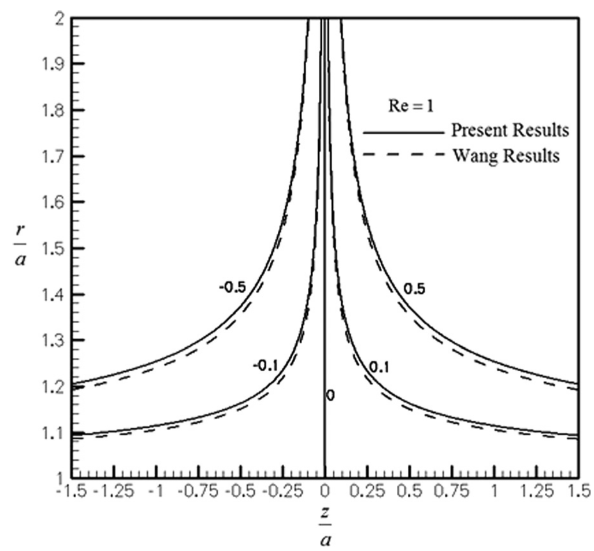

Fig. 17 The normalized stream function $\hat{\psi} = \psi/0.5\bar{k}a^3 = 2f(\eta)(z/a)$ with, Re = 1, $\alpha = 0$. Fluid is injected from the outer cylinder at $\eta = 2$ toward the inner cylinder.

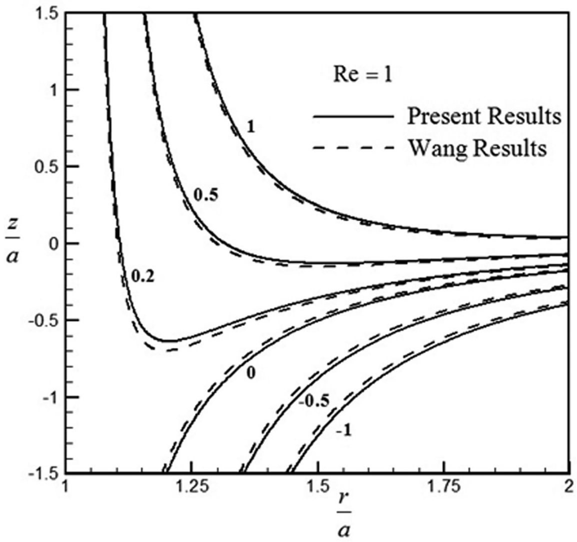

Fig. 18 The normalized stream function $\hat{\psi} = (\psi/0.5\bar{k}a^3) = 2f(\eta)(z/a) - \alpha\int_1^{\eta} H/V d\eta$ with Re = 1. Fluid is injected from the outer cylinder at $\eta = 2$ toward the inner cylinder.

6 Conclusions

Exact solution of the Navier–Stokes equations and energy equation have been presented for the steady-state viscous, flow and also heat transfer in the vicinity of an axisymmetric stagnation-point of a cylinder moving axially with a constant velocity. Here, fluid with temperature-dependent density is considered. A reduction of these equations has been obtained by use of appropriate transformations. The general self-similar solution has been obtained when the wall temperature of the cylinder or its wall heat flux was constant. All the solutions above have been presented for Reynolds numbers ranging from 0.1 to 1000, low Mach number, selected values of compressibility factor, and different values of Prandtl numbers. Shear stress has been presented as well. The axial movement of the cylinder does not have any effect on the heat transfer but the axial component of fluid velocity field increases as the speed of this movement increases. The axial component of the fluid velocity field for a specified axial velocity of the cylinder decreases as Reynolds number or compressibility factor or surface temperature or surface heat flux increases and this decrease in all cases is larger when cylinder moves faster. It is worth mentioning that in each case incompressible fluid produces the largest amount of change in axial component of the fluid velocity field. On the contrary, the axial component of the fluid velocity field increases as Prandtl number increases and this increase is larger when cylinder moves faster. Also cylinder axial speed increases the absolute value of the shear stress and the amount of this shear stress is the least for the case of incompressible fluid.

Nomenclature

a = cylinder radius
$c(\eta)$ = density ratio
$f(\eta)$ = function of η
$H(\eta)$ = function of η
k = thermal conductivity
$\bar{k}$ = freestream strain rate
Nu = Nusselt number
p = fluid pressure
P = nondimensional pressure
Pr = Prandtl number
q_w = heat flux at the wall
r, z = cylindrical coordinates
$\mathrm{Re} = \bar{k}a^2/2\upsilon$ = Reynolds number
T = temperature
T_w = wall temperature
T_∞ = freestream temperature
u = radial component of the velocity
V = axial velocity of the cylinder
w = axial component of the velocity

Greek Symbols

β = compressibility factor
$\Gamma(\eta)$ = function related to density
η = similarity variable
$\theta(\eta)$ = nondimensional temperature
μ = viscosity
υ = kinematic viscosity
$\rho(\eta)$ = fluid density
ρ_∞ = freestream density
σ = shear stress
$\hat{\psi} = \psi/0.5\bar{k}a^3 = 2f(\eta)\,(z/a) - \alpha\int_1^{\eta}(H/V)d\eta$ = normalized stream function

References

[1] Hiemenz, K., 1911, "Die Grenzchicht an Einem in den Gleichformingen Flussigkeitsstrom Eingetauchten Geraden KreisZylinder," Dinglers Polytechnic J., **326**, pp. 321–410.
[2] Homann, F. Z., 1936, "Der Einfluss Grosser Zahighkeit bei der Strmung um den Zylinder und um die Kugel," Z. Angew. Math. Mech., **16**(3), pp. 153–164.
[3] Howarth, L., 1951, "The Boundary Layer in Three-Dimensional Flow. Part II—The Flow Near Stagnation Point," Phios. Mag., **42**(335), pp. 1433–1440.
[4] Davey, A., 1961, "Boundary Layer Flow at a Saddle Point of Attachment," J. Fluid Mech., **10**(4), pp. 593–610.
[5] Wang, C. Y., 1974, "Axisymmetric Stagnation Flow on a Cylinder," Q. Appl. Math., **32**, pp. 207–213.
[6] Wang, C. Y., 1973, "Axisymmetric Stagnation Flow Towards a Moving Plate," Am. Inst. Chem. Eng. J., **19**(5), pp. 1080–1082.
[7] Gorla, R. S. R., 1976, "Heat Transfer in an Axisymmetric Stagnation Flow on a Cylinder," Appl. Sci. Res., **32**(5), pp. 541–553.
[8] Gorla, R. S. R., 1977, "Unsteady Laminar Axisymmetric Stagnation Flow Over a Circular Cylinder," Development Mech., **9**, pp. 286–288.
[9] Gorla, R. S. R., 1978, "Nonsimilar Axisymmetric Stagnation Flow on a Moving Cylinder," Int. J. Sci., **16**(6), pp. 397–400.
[10] Gorla, R. S. R., 1978, "Transient Response Behavior of an Axisymmetric Stagnation Flow on a Circular Cylinder Due to Time-Dependent Free Stream Velocity," Lett. Appl. Eng. Sci., **16**(7), pp. 493–502.
[11] Gorla, R. S. R., 1979, "Unsteady Viscous Flow in the Vicinity of an Axisymmetric Stagnation-Point on a Cylinder," Int. Sci., **17**(1), pp. 87–93.
[12] Cunning, G. M., Davis, A. M. J., and Weidman, P. D., 1998, "Radial Stagnation Flow on a Rotating Cylinder With Uniform Transpiration," J. Eng. Math., **33**(2), pp. 113–128.
[13] Grosch, C. E., and Salwen, H., 1982, "Oscillating Stagnation-Point Flow," Proc. R. Soc. London, **A384**(1786), pp. 175–190.
[14] Takhar, H. S., Chamkha, A. J., and Nath, J., 1999, "Unsteady Axisymmetric Stagnation-Point Flow of a Viscous Fluid on a Cylinder," Int. J. Eng. Sci., **37**(15), pp. 1943–1957.
[15] Saleh, R., and Rahimi, A. B., 2004, "Axisymmetric Stagnation-Point Flow and Heat Transfer of a Viscous Fluid on a Moving Cylinder With Time-Dependent Axial Velocity and Uniform Transpiration," ASME J. Fluids Eng., **126**(6), pp. 997–1005.
[16] Rahimi, A. B., and Saleh, R., 2007, "Axisymmetric Stagnation-Point Flow and Heat Transfer of a Viscous Fluid on a Rotating Cylinder With Time-Dependent Angular Velocity and Uniform Transpiration," ASME J. Fluids Eng., **129**(1), pp. 106–115.
[17] Rahimi, A. B., and Saleh, R., 2008, "Similarity Solution of Unaxisymmetric Heat Transfer in Stagnation-Point Flow on a Cylinder With Simultaneous Axial and Rotational Movements," ASME J. Heat Transfer, **130**(5), p. 054502.
[18] Shokrgozar Abbasi, A., and Rahimi, A. B., 2009, "Non-Axisymmetric Three-Dimensional Stagnation-Point Flow and Heat Transfer on a Flat Plate," ASME J. Fluids Eng., **131**(7), p. 074501.
[19] Shokrgozar Abbasi, A., and Rahimi, A. B., 2009, "Three-Dimensional Stagnation-Point Flow and Heat Transfer on a Flat Plate With Transpiration," J. Thermophys. Heat Transfer, **23**(3), pp. 513–521.
[20] Shokrgozar Abbasi, A., Rahimi, A. B., and Niazman, H., 2011, "Exact Solution of Three-Dimensional Unsteady Stagnation Flow on a Heated Plate," J. Thermodyn. Heat Transfer, **25**(1), pp. 55–58.
[21] Shokrgozar Abbasi, A., and Rahimi, A. B., 2012, "Investigation of Two-Dimensional Stagnation-Point Flow and Heat Transfer Impinging on an Accelerated Flat Plate," ASME J. Heat Transfer, **134**(6), p. 064501.
[22] Shokrgozar Abbasi, A., and Rahimi, A. B., 2013, "Solidification of Two-Dimensional Viscous, Incompressible Stagnation Flow," ASME J. Heat Transfer, **135**(7), p. 072301.
[23] Karwe, M. V., and Jaluria, Y., 1988, "Fluid Flow and Miaxed Convection Transport From a Plate in Rolling and Extrusion Process," ASME J. Heat Transfer, **110**(3), pp. 655–661.

[24] Kang, B. H., Yoo, J., and Jaluria, Y., 1994, "Experimental Study of the Convective Cooling of a Heated Continuously Moving Material," ASME J. Heat Transfer, **116**(1), pp. 199–208.
[25] Choudhury, S. R., and Jaluria, Y., 1994, "Forced Corrective Heat Transfer From a Continuously Loving Heated Cylindrical Rod in Materials Processing," ASME J. Heat Transfer, **116**(3), pp. 724–734.
[26] Karwe, M. V., and Jaluria, Y., 1991, "Numerical Simulation of Thermal Transport Associated With a Continuously Moving Flat Sheet in Material Processing," ASME J. Heat Transfer, **113**(3), pp. 612–619.
[27] Wang, C. Y., and Chiu-On, Ng., 2013, "Stagnation Flow on a Heated Vertical Plate With Surface Slip," ASME J. Heat Transfer, **135**(7), p. 074505.
[28] Hong, L., and Wang, C. Y., 2009, "Annular Axisymmetric Stagnation Flow on a Moving Cylinder," Int. J. Eng. Sci., **47**(1), pp. 141–152.
[29] Memon, N., and Jaluria, Y., 2011, "Flow Structure and Heat Transfer in a Stagnation Flow CVD Reactor," ASME J. Heat Transfer, **133**(8), p. 082501.
[30] Hayat, T., Anwar, M. S., Farooq, M., and Alsaedi, A., 2014, "MHD Stagnation Point Flow of Second Grade Fluid Over a Stretching Cylinder With Heat and Mass Transfer," Int. J. Nonlinear Sci. Numer. Simul, **15**(6), pp. 365–376.
[31] Bono, G., and Awruch, A. M., 2008, "An Adaptive Mesh Strategy for High Compressible Flows Based on Nodal Re-Allocation," J. Braz. Soc. Mech. Sci. Eng., **30**(3), pp. 189–195.
[32] Subhashini, S. V., and Nath, G., 1999, "Unsteady Compressible Flow in the Stagnation Region of Two-Dimensional and Axisymmetric Bodies," Acta Mech., **134**(3), pp. 135–145.
[33] Kumari, M., and Nath, G., 1980, "Unsteady Compressible 3-Dimensional Boundary Layer Flow Near an Axisymmetric Stagnation Point With Mass Transfer," Int. J. Eng. Sci., **18**(11), pp. 1285–1300.
[34] Kumari, M., and Nath, G., 1981, "Self-Similar Solution of Unsteady Compressible Three-Dimensional Stagnation-Point Boundary Layers," J. Appl. Math. Phys., **32**(3), pp. 267–276.
[35] Katz, A., 1972, "Transformations of the Compressible Boundary Layer Equations," SIAM J. Allied Math., **22**(4), pp. 604–611.
[36] Afzal, N., and Ahmad, S., 1975, "Effect of Suction and Injection on Self-Similar Solutions of Second-Order Boundary Layer Equations," Int. J. Heat Mass Transfer, **18**(5), pp. 607–614.
[37] Libby, P. A., 1967, "Heat and Mass Transfer at a General Three-Dimensional Stagnation Point," AIAA J., **5**(3), pp. 507–517.
[38] Gersten, K., Papenfuss, H. D., and Gross, J. F., 1978, "Influence of the Prandtl Number on Second-Order Heat Transfer Due to Surface Curvature at a Three-Dimensional Stagnation Point," Int. J. Heat Mass Transfer, **21**(3), pp. 275–284.
[39] Mozayyeni, H. R., and Rahimi, A. B., 2013, "Three-Dimensional Stagnation Flow and Heat Transfer of a Viscous, Compressible Fluid on a Flat Plate," ASME J. Heat Transfer, **135**(10), p. 101702.
[40] Mozayyeni, H. R., and Rahimi, A. B., 2014, "Unsteady Two-Dimensional Stagnation-Point Flow and Heat Transfer of a Viscous, Compressible Fluid on an Accelerated Flat Plate," ASME J. Heat Transfer, **136**(4), p. 041701.
[41] Mohammadiun, H., and Rahimi, A. B., 2012, "Axisymmetric Stagnation-Point Flow and Heat Transfer of a Viscous, Compressible Fluid on a Cylinder," J. Thermophys. Heat Transfer, **26**(3), pp. 494–502.
[42] Press, W. H., Flannery, B. P., Teukolsky, S. A., and Vetterling, W. T., 1997, *Numerical Recipes, the Art of Scientific Computing*, Cambridge University Press, Cambridge, UK.